Hybrid Silica−PVA Nanofibers via Sol−Gel Electrospinning

Tahira Pirzada,[†,§] Sara A. Arvidson,[‡,§] Carl D. Saquing,*[,‡,⊥] S. Sakhawat Shah,[†] and Saad A. Khan*[,‡]

[†]Department of Chemistry, Quaid-i-Azam University, Islamabad, 44000, Pakistan
[‡]Department of Chemical and Biomolecular Engineering, North Carolina State University, Raleigh, North Carolina 27695-7905, United States

ⓢ *Supporting Information*

ABSTRACT: We report on the synthesis of poly(vinyl alcohol) (PVA)−silica hybrid nanofibers via sol−gel electrospinning. Silica is synthesized through acid catalysis of a silica precursor (tetraethyl orthosilicate (TEOS) in ethanol−water), and fibers are obtained by electrospinning a mixture of the silica precursor solution and aqueous PVA. A systematic investigation on how the amount of TEOS, the silica−PVA ratio, the aging time of the silica precursor mixture, and the solution rheology influence the fiber morphology is undertaken and reveals a composition window in which defect-free hybrid nanofibers with diameters as small as 150 nm are obtained. When soaked overnight in water, the hybrid fibers remain intact, essentially maintaining their morphology, even though PVA is soluble in water. We believe that mixing of the silica precursor and PVA in solution initiates the participation of the silica precursor in cross-linking of PVA so that its −OH group becomes unavailable for hydrogen bonding with water. FTIR analysis of the hybrids confirms the disappearance of the −OH peak typically shown by PVA, while formation of a bond between PVA and silica is indicated by the Si−O−C peak in the spectra of all the hybrids. The ability to form cross-linked nanofibers of PVA using thermally stable and relatively inert silica could broaden the scope of use of these materials in various technologies.
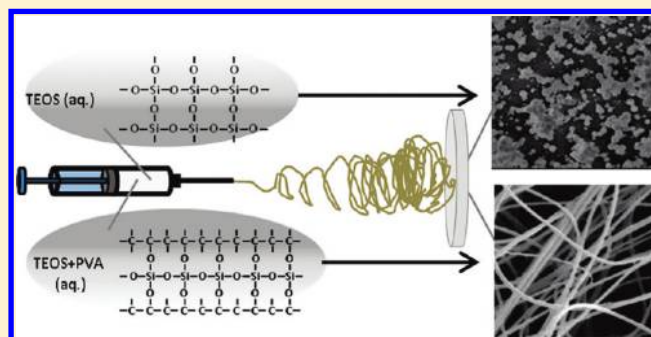
1. INTRODUCTION

Organic−inorganic hybrids are important in a variety of fields as they combine the desirable properties of the inorganic phase (thermal stability, rigidity) with that of the organic phase (flexibility, processability, ductility).[1,2] In recent years, polymer−silica hybrids with enhanced thermal and mechanical properties[2] (because of the silica component), better flexibility (due to the polymer content), and various tailored properties have attracted a lot of attention for a variety of applications including catalysis,[3] adsorption,[4] pervaporation,[5,6] sensors,[7] and enzyme encapsulation.[8] The scope and utility of these polymer−silica hybrids can be further broadened by transforming them to nanofibrous structures that exhibit high surface area to volume ratios.[2−4,9,10]

Of the various approaches developed to synthesize polymer−silica hybrid nanofibers, the one-step electrospinning process has received a lot of attention due to its simplicity, cost effectiveness, and speed.[2,4,11] Electrospinning is a decades-old technique which draws very fine fibers from a viscous liquid (usually a polymer solution or polymer melt) under the force of an electrostatic field.[12−16] The resulting fibers have a high surface area to volume ratio that makes them potential candidates for a variety of fields such as membrane technology,[17] drug delivery systems,[18] enzyme immobilization,[19] electronics,[20] and sensors.[21] Combining electrospinning with sol−gel processing provides a way to fabricate one-dimensional nanostructures with tailorable morphologies, size, and composition.[22]

During the last few decades, the sol−gel method has been widely used to prepare a variety of silica-based materials in forms such as monoliths, powders, tubes, and fibers.[23,24] A typical sol−gel process consists of catalyzed hydrolysis and condensation of an initially small molecule (usually an alkoxide) leading to its transformation to an intricate, highly viscous polymeric network and then ultimately resulting in the formation of a 'gel' (Scheme I in the Supporting Information). Depending on the composition of the solution and the reaction conditions, the transformation of the sol to the gel state can be modified application requirements.[23−25] Since the solution continues to gel over time, there may be only a certain window of time in which the partially gelled solution may be electrospun. Previously, silica nanofibers have been reported from tetraethyl orthosilicate (TEOS) based sol−gels either by pulling the fibers from a sufficiently viscous sol−gel[9] or by dry spinning.[10] Reports of electrospinning of this type of sol−gel are few, owing to the difficulty of electrospinning a solution that lacks polymer entanglements, and has led to combined sol−gel synthesis/electrospinning with gelators or binders[2,4,26−28] to obtain ceramic fibers in the 200−600 nm

range.[3,4,26−28] Limited results on electrospun silica nanofibers from a precursor mixture containing TEOS, ethanol, and HCl without any added polymer have also been reported,[26] but a systematic study of the variation in properties of the electrospinning solution on the structure of electrospun fibers is not reported. In 2010, Xu et al. provided an account of the synthesis of hybrid silica−yttria and silica−zirconia−yttria fibers through sol−gel electrospinning using a small amount (1−1.5%) of polyethylene oxide (PEO) as a carrier polymer.[27] They examined the changing viscosity of the sol−gel mixture with the passage of time and used a narrow range of solution viscosity (0.3−0.4 Pa s) to produce nonbeaded fibers. However, their objective was to generate dense ceramic nanofibers which were obtained by calcining the polymer content from the nanofibers.

Poly(vinyl alcohol) (PVA) is an easily electrospun polymer that can be used as the organic phase of the polymer−silica hybrid fibers. Its biocompatibility, processability, and hydrophilicity[29,30] have led to its industrial use in areas such as membranes,[31] adhesives,[32] paints, and coatings.[30] Water solubility, however, limits PVA use in applications such as ultrafiltration, catalyst support, or biomedical engineering, which require stability in aqueous systems. Research groups are working on chemical or physical cross-linking of PVA to reduce its water solubility using different agents and processes.[33−39] Chemical cross-linkers including glutaraldehyde,[35,36,39] hexamethylene diisocyante,[33] and maleic acid[40] have been used by various research groups to bind the terminal hydroxyl groups of PVA which are mainly responsible for its hydrophilicity;[33,35] however, most of these approaches are found to render the material toxic or thermally unstable. Photocross-linking[34] and freezing−thawing cyclic processing[29,37] of PVA offer approaches which produce cross-linked PVA that is nontoxic, but the products are mostly thermally unstable, and the processing requires considerable time and energy expenditures.[29,36−39] Therefore, there is a need to develop a PVA composite with reduced water solubility while maintaining the inherent nontoxicity of PVA through a cost-effective approach.

Using electrospinning and sol−gel methodologies, we report a method to prepare silica−PVA composite nanofibers possessing a nonintuitive property of minimal water solubility and provide a description of the molecular interactions to explain the limited solubility of the resulting nanofibers. Since silica is biocompatible, thermally stable, and comparatively inert, incorporation of silica with PVA may produce hybrids with enhanced thermal and chemical stability without relinquishing the biocompatibility of PVA.[41,42] Silanol groups on the silica surface (Scheme I in the Supporting Information) are capable of reducing the water solubility of PVA by developing stronger intermolecular interactions, which may result in the improved stability of the hybrid fibers in humid/aqueous environments. Although there is some work already reported on the synthesis of PVA-templated silica, few research groups have synthesized PVA−silica nanofibers using silicon alkoxide as the precursor.[2−4,43,44] In most of the cases, colloidal silica particles were used as the silica source.[45,46] Generally, PVA was used to increase the number of entanglements in the silica-containing solution and was later removed to make porous silica fibers;[8,47] in cases where PVA was not removed from the hybrid PVA−silica fibers,[3,5] the effect of silica on the solubility of PVA was not thoroughly investigated.[5,43] Our focus is to spin fibers from solutions containing PVA and a silica

precursor (TEOS) in different ratios as we believe that the proportion of PVA to silanols may affect the ability to form a network; without this network, the solution will not electrospin due to a lack of entanglements. Moreover, by varying the ratio of TEOS:PVA, we can also determine the concentration range of TEOS and PVA in the electrospinning solution that provide high-quality fibers with improved thermal stability, reduced defects, and reduced sensitivity to humid/aqueous conditions. Because of the time dependence of gelation, we studied the effect of aging time of the sol−gel process prior to adding the PVA, which was helpful to conclude whether the silica network or the TEOS is responsible for cross-linking the PVA. Some groups have observed the reduced water solubility of the PVA−silica hybrids,[2,6,48] but to our knowledge, no one has studied the morphology and chemistry of water-soaked PVA−silica hybrid fibers in detail or related the changing characteristics (e.g., viscosity, surface tension, conductivity) of the system with the fiber morphology. Fibers are analyzed in their as-spun state and after soaking them in deionized water for 24 h, which we believe is important for, first, understanding the interactions between the silica and the PVA occurring in the system during both the sol−gel transformation and electrospinning and, second, relating those interactions to the stability of the hybrid fibers in aqueous systems. The possible increase in the stability of the hybrid fibers in aqueous systems will make them a suitable candidate for applications in fields such as ultrafiltration, tissue engineering, and catalysis.

2. MATERIALS AND METHODS

2.1. Materials. Tetraethyl orthosilicate (TEOS 99%), hydrochloric acid (HCl 37%), and PVA (weight-average molecular weight 205 000 Da, 88% hydrolyzed) were supplied by Sigma-Aldrich. Ethanol (C_2H_5OH) was purchased from Fisher Chemicals. Deionized water was used throughout the experiments. All chemicals were used as received without further purification. PVA (7 wt %) was dissolved in deionized water at 60 °C while stirring. TEOS solutions ranging from 10 to 70 wt % were made by dissolving TEOS in ethanol and deionized water in a molar ratio of x:3:7 TEOS:ethanol:water, where x was between 1.11 and 23.3, and then adding HCl dropwise to reach a solution concentration of 0.1 M followed by stirring at 60 °C for 1 h or more. Afterward, the PVA solution was gradually added to the TEOS solution, and the mixture was thoroughly mixed for 1 h by stirring at 60 °C. After selecting the TEOS concentration that gave fibers with the least beads and smallest fiber diameter, TEOS was mixed with water, ethanol, and HCl at a molar ratio of 1:3:8:0.04 and stirred at 60 °C for 1 h unless otherwise specified. After 1 h, the PVA solution was added. The resulting solutions were stirred for 1 h at 60 °C after the addition of PVA. The compositions and nomenclatures of all solutions are provided in Tables 1 and 2.

Table 1. TEOS and PVA Concentration in Electrospun Solutions and the Resulting Fiber Diameters (with standard deviation of 100 measurements)

TEOS wt % in solution	silica wt % in the solution	PVA wt % in the solution	silica:PVA ratio in solution (by wt)	fiber diameter (nm)
5	1.4	3.5	2:5	48 ± 20
10	2.8	3.5	4:5	50 ± 20
15	4.2	3.5	6:5	100 ± 30
20	5.6	3.5	8:5	150 ± 30
25	7.0	3.5	10:5	400 ± 100
30	8.4	3.5	12:5	330 ± 90
35	9.8	3.5	14:5	330 ± 130

Table 2. Sample Nomenclature and Fiber Sizes with the Surface Tension, Viscosity, Conductivity of Solutions, and Weight Loss by TGA of Fibers Electrospun from Given Solution

sample	TEOS solution:PVA solution	TEOS:PVA ratio (by wt) in solution	TEOS aging time (h)	PVA wt % in the solution	silica:PVA ratio (by wt) in solution	fiber diameter (nm)	viscosity (Pa S)	surface tension (dyn/cm)	conductivity (mS)
TP$_{105}$	TEOS solution only (40 wt %)		5			140 ± 60^{a}	0.004	29.0	3.6
TP$_{411a}$	4:1 (as-spun)	160:7	1	1.4	45:7	150 ± 30	0.020	29.0	4.2
TP$_{411s}$	4:1 (soaked)	160:7	1	1.4	45:7	150 ± 60			
TP$_{412a}$	4:1 (as-spun)	160:7	2	1.4	45:7	380 ± 130			
TP$_{412s}$	4:1 (soaked)	160:7	2	1.4	45:7	300 ± 60			
TP$_{413a}$	4:1 (as-spun)	160:7	3	1.4	45:7	470 ± 130			
TP$_{413s}$	4:1 (soaked)	160:7	3	1.4	45:7	330 ± 95			
TP$_{414a}$	4:1 (as-spun)	160:7	4	1.4	45:7	650 ± 190	0.020		
TP$_{414s}$	4:1 (soaked)	160:7	4	1.4	45:7	550 ± 140			
TP$_{321a}$	3:2 (as-spun)	60:7	1	2.8	17:7	240 ± 90	0.063	31.0	5.8
TP$_{321s}$	3:2 (soaked)	60:7	1	2.8	17:7	370 ± 50			
TP$_{111a}$	1:1 (as-spun)	40:7	1	3.5	11:7	310 ± 60	0.091	32.7	5.9
TP$_{111s}$	1:1 (soaked)	40:7	1	3.5	11:7	320 ± 60			
TP$_{231a}$	2:3 (as-spun)	27:7	1	4.2	5:7	360 ± 150	0.131	37.8	6.0
TP$_{231S}$	2:3 (soaked)	27:7	1	4.2	5:7	340 ± 70			
TP$_{141a}$	1:4 (as-spun)	10:7	1	5.6	3:7	230 ± 70	0.250	42.8	6.6
TP$_{141s}$	1:4 (soaked)	10:7	1	5.6	3:7				
TP$_{010}$	PVA only (7 wt %)		1	7		220 ± 30	0.323	45.8	232.1

^{a}TP$_{105}$ produced particles instead of fibers. Therefore, sizes in the fiber diameter column indicate particle diameter for TP$_{105}$.
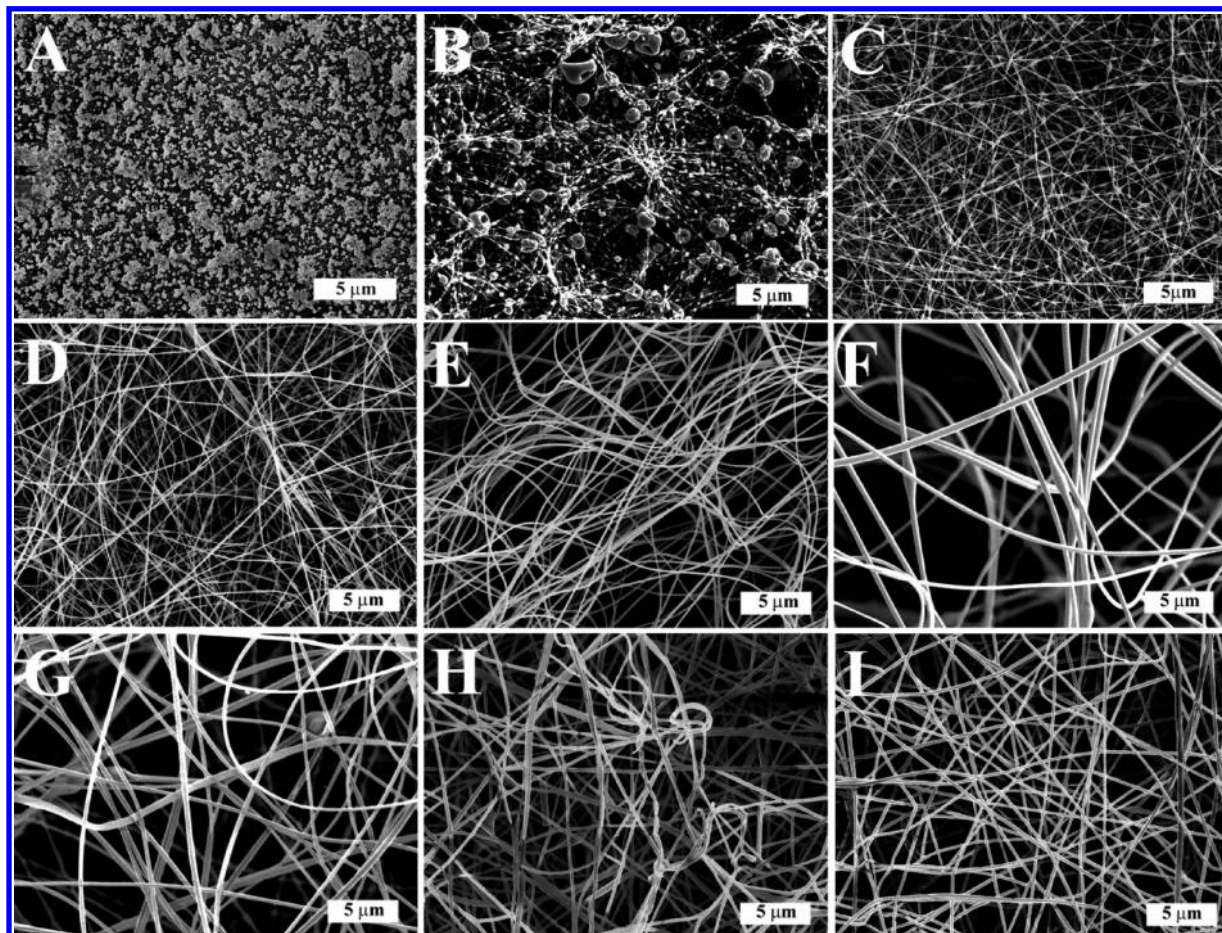

Figure 1. As-spun (A) 40% TEOS solution aged 5 h (no PVA), (B) 3.5% PVA and 5% TEOS, (C) 3.5% PVA and 10% TEOS, (D) 3.5% PVA and 15% TEOS, (E) 3.5% PVA and 20% TEOS, (F) 3.5% PVA and 25% TEOS, (G) 3.5% PVA and 30% TEOS, (H) 3.5% PVA and 35% TEOS, and (I) 7% PVA solution (no TEOS).

2.2. Electrospinning. A variable high-voltage power supply (Gamma High Voltage Research, D-ES-30PN/M692) was used to provide voltage to the electrospinning solution. The solution was loaded in a 10-mL syringe with a stainless steel capillary metal hub needle. The positive electrode of the power supply was attached to the needle tip, while the grounded electrode was connected to a metallic collector wrapped with aluminum foil. All fibers were spun at 20 kV keeping a constant tip-to-collector distance (TCD) of 10 cm. The flow rate was kept at 0.5 mL/h throughout.

2.3. Sample Characterization. The surface morphology and fiber diameter of the samples were analyzed by scanning electron microscopy. A FEI XL30 SEM-FEG was used to obtain images of gold sputter-coated nanofibers at 5 kV. The coating was performed with a K-550X sputter coater to reduce charging of the electrospun sample. Image J software was used to determine the average fiber diameter and standard deviation by measuring the diameter of at least 100 fibers.

Infrared (IR) spectra of the composite fibers were recorded with a Nicolet 560 FTIR spectrometer in transmittance mode at room temperature. All samples were scanned from 4000 to 400 cm^{-1} with a resolution of 4 cm^{-1}. Spectra were taken from an average of 32 scans for each sample. Data acquisition was done through OMNIC software.

A TA-Hi-Res 2950 thermal gravimetric analyzer was used to determine the weight loss dynamics of the fibers from room temperature to 850 °C at a heating rate of 10 °C/min in a nitrogen environment. To check the solubility of the fiber in water, the protocol established by Shao et al.[2] and Tang et al.[35] was followed and fiber mats were submerged in deionized water at room temperature for 24 h and then vacuum dried overnight for removal of trace amounts of water before their surface morphology, thermal, and structural properties were analyzed.

Steady state rheological experiments were performed on selected samples as a function of time at 25 °C with an AR-G2 Rheometer using a 40-mm diameter, 2° cone, and plate geometry with solvent trap. The rheometer was operated in stiff bearing mode for PVA solutions, while all others were measured in soft mode because of their low viscosity. The shear stress was varied between 0.1 to 20 Pa for all experiments.

A 2-probe Accumet Basic AB30 conductivity meter by Fisher Scientific was used to measure the conductivity of the solutions, and surface tension was measured with a DuNouy interfacial tensiometer CSC.

3. RESULTS AND DISCUSSION

3.1. Effect of Silica Concentration and PVA:Silica Ratio on Composite Fiber Morphology. Figure 1 shows SEM micrographs of samples generated after electrospinning from solutions containing silica precursor in different concentrations with PVA. Silica precursor (TEOS solution containing HCl, ethanol, and water) gives only nanoparticles having an average diameter of 140 ± 60 nm (Figure 1A), even when allowed to age for 5 h. Clearly, the high viscosity resulting from gelation of the silica precursor is not sufficient alone to produce electrospun fibers. (The effect of aging time on the viscosity of TEOS is discussed in more detail below.) Unlike the TEOS solution, the PVA solution gives fibers with no beads and a narrow fiber size distribution (220 ± 30 nm, Figure 1I). By blending PVA into the silica precursor solution after only 1 h of aging, fibers are obtained (Figure 1B−H) in all cases of silica−PVA blends. In Figure 1, the solution being electrospun contained 3.5 wt % PVA while the TEOS concentration varied (the concentrations of TEOS and PVA in the electrospun solutions are reported in Table 1). Fiber diameters are small, and the fibers are highly beaded at very low concentrations of TEOS, which indicates the inability of the jet to undergo extensional flow.[49] With an increase in TEOS concentration to 20 wt %, good-quality fibers are obtained which can be

attributed to the increased percentage of the viscous silica network in the precursor mixture. On further increase of silica concentration, the bead defects return (Figure 1F) and the fiber diameters increase in size and nonuniformity. The larger fiber diameter is a result of the increased viscosity of the solution, while defects are likely a result of the decreased conductivity of the solution. A more thorough investigation into the effect of these parameters with electrospinnability is presented below.

It has been shown that electrospinning PVA at concentrations above 6 wt % results in nonbeaded fibers.[35] To study the effect of varying PVA content on the PVA−silica hybrid fiber morphology, TEOS−PVA solutions with 1.4−5.6 wt % PVA (equivalent to a TEOS:PVA mass ratio ranging from 4:1 to 1:4) were electrospun. Table 2 lists the amount of TEOS and PVA in each solution as well as the fiber diameters resulting from electrospinning each solution, whereas Figure 2 shows SEM images of representative nanofiber samples. The first two digits of the subscript of each sample name indicate the ratio of

Figure 2. As-spun fibers with TEOS solution:PVA solution equal to (A) 4:1 (TP$_{411a}$), (B) 3:2 (TP$_{321a}$), (C) 1:1 (TP$_{111a}$), (D) 2:3 (TP$_{231a}$), and (E) 1:4 (TP$_{141a}$). Composite fiber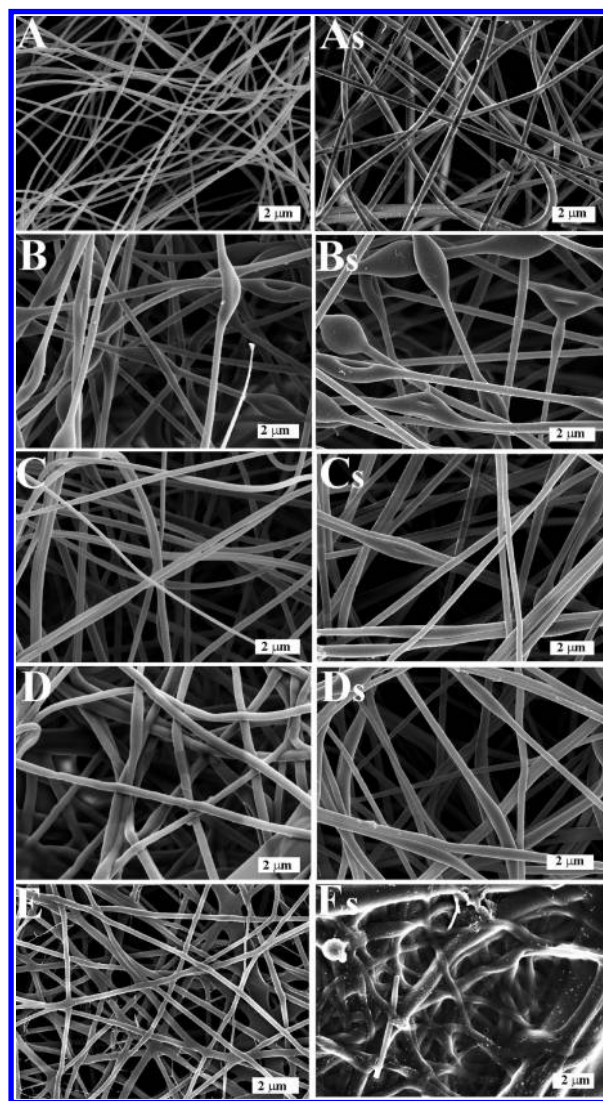s after a 24-h soak in deionized water and subsequent drying under vacuum with TEOS solution:PVA solution equal to (As) 4:1 (TP$_{411s}$), (Bs) 3:2 (TP$_{321s}$), (Cs) 1:1 (TP$_{111s}$), (Ds) 2:3 (TP$_{231s}$), and (Es) 1:4 (TP$_{141s}$).

TEOS solution to PVA solution, while the third digit is the aging time of the TEOS solution in hours (i.e., TP_{141} contains 1:4 TEOS solution to PVA solution by mass, while TEOS was aged for 1 h before mixing with PVA). With an increase in the PVA content in the electrospun solution from 1.4% to 3.5% (TP_{411} to TP_{111}), the fiber size increases (Figures 2A−C; Table 2), but with a further increase in PVA content to 4.2% the fiber diameters are approximately constant (Figure 2D; Table 2) before decreasing slightly at 5.6% PVA content (Figure 2E; Table 2). The number of bead defects was the greatest for sample TP_{321}, while flattened, fused fibers were observed for TP_{141}. According to Koski et al.[49] and Tang et al.,[35] at higher molecular weights, due to reduced solvent evaporation and increased solution viscosity, relatively wet fibers flatten upon impact with the collector. The flattened, fused fibers can be attributed to the high molecular weight of the electrospinning solution that can be a result of either the increased solution viscosity due to higher polymer content or the cross-linking between PVA and silica during the aging process. Since a thorough investigation of the viscosity of the precursor mixtures can give us an idea about what is happening inside the solution, Figure 3 shows the viscosity of solutions with
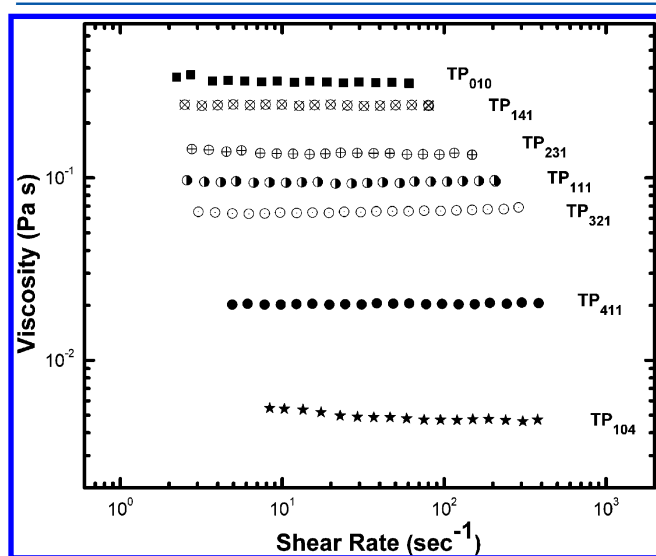
viscosity of the TP_{141} solution (Figure 3) indicates that this ratio of TEOS:PVA results in a higher molecular weight of the silanol/silica/PVA network, which leads to the flattened morphology of the fibers. It is evident from Figure 1I that flattened fibers are not observed when PVA is spun in the absence of TEOS, despite its higher viscosity (Figure 5b), a property that can be attributed to the comparatively lower molecular weight of the PVA compared to the silica–PVA possibly cross-linked network. Note that the blended solution viscosities are not well predicted by a standard, inverse, or log rule of mixture (Table 3) that predicts blend viscosity based on the viscosity of the constituent parts. The lack of adherence to any of the listed rules of mixture suggests that PVA and silica may interact in solution, as simple blending would have resulted in a viscosity that was a direct combination from both constituents.

Other than the viscosity, the surface tension and conductivity of a solution also dictate its ability to electrospin, with higher surface tension, leading to bead defects in fibers.[12] The surface tension of TEOS−PVA solutions increases with increasing PVA content (Table 2); however, the presence of beads did not correlate with the lower surface tension, which can be seen in Figure 2 by comparing the fiber morphology of samples TP_{321} and TP_{111}, which have lower surface tension, to samples TP_{231} and TP_{141}, which have higher surface tension. It appears that the increase in conductivity (Table 2), which is caused by a greater percentage of PVA, plays a greater role in reducing Raleigh instability and facilitates formation of defect-free fibers despite the rise in surface tension.

3.2. Effect of Silica Precursor Aging Time. Since the number of silica networks in the gelling TEOS increases with the passage of time,[24] we investigated how the degree of gelling affects the silica−PVA hybrids by allowing TEOS to gel for a period ranging from 1 to 4 h and then thoroughly mixing it with the PVA solution before electrospinning. Electrospinning of the mixtures containing TEOS sol aged for periods longer than 4 h is not reported in this work since such electrospinning mixtures were too viscous or gel-like to be electrospun. Also note that when a mixture containing PVA and TEOS (not aged) was thoroughly mixed and immediately electrospun, it resulted in formation of a mixture of fibers and droplets (Supporting Information, Figure 1). After about 2 h, the mixture started to block the nozzle and thick fibers started forming visible from the tip of the needle to the collector (Supporting Information, Figure 2). Such a small window of operation was also observed when aged TEOS was mixed with PVA and followed as a function of time, thereby also prompting us to examine the effect of TEOS aging rather than that of the temporal behavior of the mixed system.

Figure 3. Log−log plot of viscosities of solutions containing 7% PVA with no TEOS (TP_{010}), 40% TEOS solution aged for 4 h with no PVA (TP_{104}), and blends of 7% PVA and 40% TEOS in varying proportions (TP_{141}−TP_{411}) aged for 1 h.

varying TEOS:PVA. All of the PVA, TEOS, and TEOS−PVA solutions show Newtonian behavior (viscosity not a function of shear rate) over the measured range of shear rates. The higher

Table 3. Predicted and Experimental Values of Solution Viscosities

sample	TEOS solution:PVA solution	fraction PVA	fraction TEOS	predicted viscosity (Pa S)			measured viscosity (Pa s)
				S-ROM	I-ROM	L-ROM	
TP_{010}	0:1	1	0				0.323
TP_{141}	1:4	0.8	0.2	0.259	0.0191	0.134	0.25
TP_{231}	2:3	0.6	0.4	0.195	0.01	0.056	0.131
TP_{111}	1:1	0.5	0.5	0.163	0.008	0.036	0.091
TP_{321}	3:2	0.4	0.6	0.132	0.007	0.023	0.063
TP_{411}	4:1	0.2	0.8	0.068	0.005	0.01	0.02
TP_{105}	1:0	0	1				0.004

The electrospun fiber morphology varied with the TEOS aging time (Figure 4). Increased aging time resulted in the
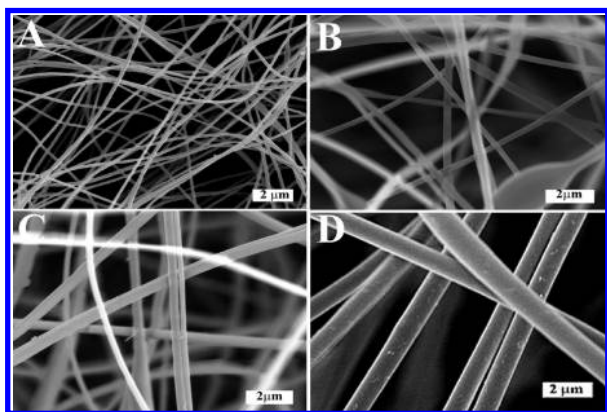

Figure 4. Fibers spun from solutions containing 4:1 TEOS:PVA. Aging time of the TEOS solution before adding the PVA solution is varied: (A) 1 (TP$_{411a}$), (B) 2 (TP$_{412a}$), (C) 3 (TP$_{413a}$), and (D) 4 h (TP$_{414a}$).

formation of fibers with larger diameters and with a broader distribution in diameter sizes (Table 2). Solution viscosity, being a measure of entanglement, have been used in the literature to explain the fiber morphology. Figure 5A shows the viscosity of TEOS and TEOS−PVA solutions after 1−4 h of aging. The increase in fiber diameter seen with aging time can be attributed to the increased viscosity of the solution with the increasing gelation time of the TEOS sol. The fiber diameters are also greater than those formed by the PVA solution without TEOS (TP$_{010}$). For shorter TEOS aging times (less than 3 h), viscosity data of the TEOS−PVA solutions was unable to explain the relationship between fiber morphology and solution viscosity since the fiber diameters increased with increasing aging time (Figure 4A and 4B) despite similar viscosities of TEOS−PVA solutions (Figure 5A). After aging for approximately 3 h, the viscosity of the TEOS−PVA mixtures exhibits a rise and non-Newtonian behavior at low shear rates, which led

to further increases in fiber diameter (Figure 4C and 4D). Although the TEOS sol converts into a viscous polymeric network gel structure (consisting of siloxane linkages in the bulk and silanol groups on the surface[24]) with the passage of time, the viscosity of the TEOS sol alone is not strongly affected by aging time and exhibits Newtonian behavior (Figure 5B). Further, it should be noted that TEOS at 4−5 h aging time does not yield fibers (Figure 1A), which indicates that the silica network cannot be electrospun on its own. This, taken with the fact that the viscosity of TEOS−PVA sol−gel mixtures increases (even above that of PVA alone) after longer TEOS aging times, suggests that the TEOS−PVA mixture has a greater effective molecular weight when a larger amount of silica has formed prior to the introduction of PVA. The rise in the effective molecular weight cannot be attributed to the silica network only, since TEOS alone does not show such a high viscosity. Therefore, the possible cross-linking of PVA by the silanol groups of the silica network can be held responsible for an increase in the viscosity of the precursor mixture due to the higher effective molecular weight. If TEOS created covalent bonds cross-linking the PVA more readily than silanols, then the opposite trend in viscosity with aging time would have resulted.

3.3. Effect of Water Exposure on Fiber Characteristics. The acid-catalyzed sol−gel processing of TEOS leads to a faster hydrolysis and slower condensation, which results in formation of a linear polymeric network gel due to chain elongation created by terminal silanol groups.[24] Therefore, the resulting silica network contains sufficient surface silanol groups available to participate in hydrogen bonding. Since PVA also has its terminal −OH groups easily available for bonding, hydrogen bonding between PVA and silica is possible which might result in formation of Type II hybrids (having stronger bonds for interfacial interactions)[1] rather than just physical blends (Type I hybrids) of silica and PVA. What is unclear is whether the silica−PVA hydrogen bonding would be the dominant interaction between the molecules or whether, as proposed in Figure 6, new covalent bonds form. If hydrogen bonding is the dominant interaction (Type I hybrids), presumably the silica−
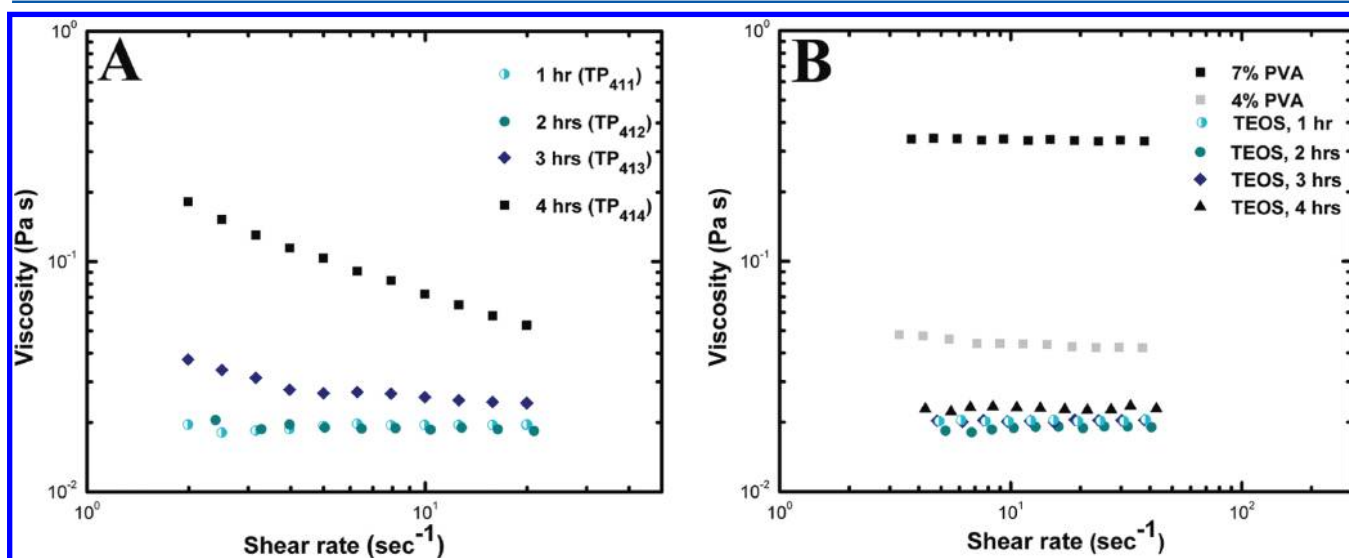

Figure 5. (A) Viscosity versus shear rate of PVA−TEOS solutions. Aging time of TEOS before adding PVA is noted (TP$_{411}$−TP$_{414}$). (B) Viscosity versus shear rate of solutions containing 4% PVA (no TEOS), 7% PVA (no TEOS), and TEOS (no PVA) solutions with the TEOS aging times noted.
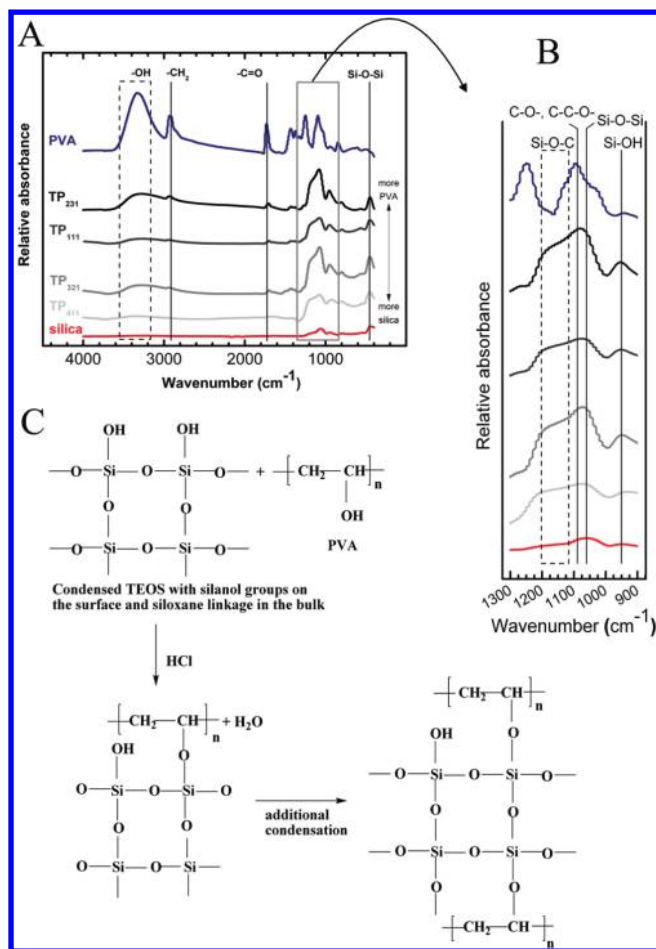
Figure 6. FTIR spectra of as-spun PVA, silica, and PVA−silica composites (A). Enlarged version (B) shows the Si−O−C peak which is generated because of the interaction between −OH groups of PVA and surface silanols of silica resulting in possible production of suggested structure (C).

PVA hybrids would dissolve or swell when exposed to water, whereas if covalent bonds formed which cross-link PVA (Type II hybrids) the PVA−silica complex would be rendered insoluble in water.

Evident from 24 h exposure to water, hybrid fibers displayed a significant decrease in solubility with the increase in silica content, i.e., weight loss of TP_{411}, TP_{321}, and TP_{111} were negligibly small ($0.02 \pm 0.001\%$, $0.03 \pm 0.002\%$, and $0.17 \pm 0.001\%$, by weight, respectively). Interestingly, although still small, the weight loss starts to increase to $0.39 \pm 0.030\%$ and $4.03 \pm 0.095\%$ when the TEOS to PVA ratio is decreased (i.e., the amount of PVA with respect to TEOS is increased) to less than 1:1, and this presumably is due to the dissolution of the excess of PVA not involved in the cross-linking. Figure 2 displays the morphology of silica−PVA hybrid fibers before (A−E) and after (A_s−E_s) submersion in deionized water for 24 h. (Morphology of pure PVA nanofiber web cannot be studied after soaking in water due to complete dissolution of the PVA nanofiber.[35]) With the exception of TP_{141} (theoretical silica:PVA of 3:7 in fiber), there were no significant changes in the morphology of the water-exposed fibers, and fiber diameters were similar before and after exposure (Table 2). Water insolubility of the silica−PVA composite structures indicates formation of covalent bonds between silica and PVA[36,49] and supports the suggested scheme of cross-linking

between silica and PVA (Figure 6C). In the case of TP_{141}, the fibers fused during exposure to water but did not fully dissolve; loss in morphology of fibers in this case can be attributed to dissolution of a fraction of PVA that was not cross-linked by the silica due to a comparatively higher content of PVA in the fiber. This suggests that there are a limited number of surface silanol groups in the silica network available to react with PVA.

3.4. FTIR Analysis of Silica and the Fibers. FTIR spectra of as-spun fibers (Figure 6) indicate which bonds are formed or lost during the sol−gel and electrospinning processes and elucidate whether silica−PVA hybrids are a physical mixture or covalently bound network. PVA shows a prominent peak around 3300 cm^{-1} due to its −OH groups.[50,51] Another characteristic peak between 1000 and 1050 cm^{-1} is assigned to the C−O−H stretching movement in aliphatic alcohols. Silica shows characteristic peaks at 1096, 820, and 483 cm^{-1} corresponding to the asymmetrical stretching, symmetric stretching, and bending vibrations in Si−O−Si bonds, respectively.[47,52]

On comparison of PVA and silica FTIR spectra with those of hybrid fibers, we find that except for silica alone all the fibers just show two PVA characteristic peaks at around 2900 and 1700 cm^{-1} which are characteristic of −CH$_2$ and C=O groups.[47] The intensities of these peaks are proportional to the PVA content in the hybrid fibers. Fully hydrolyzed PVA does not contain any C=O group, only the partially hydrolyzed PVA. The C=O group is part of the acetate groups present in the unhydrolyzed PVA, and it gets more intense with reduced degree of hydrolysis.[51] Even though 88% hydrolyzed PVA is used in this work, the C=O peak is still quite prominent in the IR spectra. Silica and all hybrid nanofibers exhibit a peak between 440 and 500 cm^{-1} and peaks between 1000 and 1100 cm^{-1} representing the typical silica peaks in the as-spun and water-soaked fibers (Supporting Information, Figure 3). The presence of Si−O−Si in the hybrid fibers indicates that adding PVA to the aged precursor does not interrupt formation of the silica network in the hybrids. The peaks characteristic of Si−O−Si in the hybrids are more intense than those in silica, which can be attributed to the asymmetry in the hybrid Si−O−Si bonds compared to the symmetry of the Si−O−Si bonds in silica alone, rather than necessarily an increase in the relative percentage of Si−O−Si in the two systems.[53] This transformation in sample symmetry indicates there may be Si−O−C bonds in the hybrids, making the sample asymmetric (Figure 6C).

Compared to the C−OH peak in PVA at 1094 cm^{-1}, the hybrid fibers give broader peaks with an increase in silica content (Figure 6A and 6B). This increase in the width of the peaks and its slight shift to higher wavenumbers can be attributed to overlapping of Si−O−Si (at approximately 1100 cm^{-1}) with the C−C−O peak (at 1096 cm^{-1}) due to the interference of C−O stretching movement of PVA with asymmetric Si−O−Si stretching.[48,52] The shoulder on the Si−O−Si peaks at around 1110 cm^{-1} can be attributed to the presence of a Si−O−C bond, which indicates formation of a new Si−O−C bond in the hybrids (Figure 6C) through cross-linking silica and PVA. A similar trend is also observed by Xu et al., who reported condensation of silanol groups with the −OH on the PVA chain to form Si−O−(PVA)−O−Si cross-links or "bridges".[54]

Although the broad bands between 3200 and 3400 cm^{-1} are from multiple origins and cannot be used to determine the exact content of the −OH group in the hybrids, these bands

can be used as a relative measure of the hydroxyl content of the hybrid fibers as compared to the −OH band in PVA alone. The relative decrease in the intensity of the −OH characteristic peak at 3300 cm^{-1} for the hybrid fibers is consistent with the decrease in PVA content in the precursor mixture. The variation in the −OH peak intensity may also be due to their involvement in the concurrent cross-linking and condensation reactions of PVA, TEOS, and silica (Figure 6C). The presence of measurable −OH peaks in the FTIR spectra of the hybrids (Figure 6A) indicates the possibility that some of the −OH groups, whether from silanol or PVA, are not consumed in cross-linking. It is germane to note that in the silica curve of Figure 6A there is a weak peak at ∼3300 cm^{-1} due to the presence of −OH, but this peak is not clearly seen due to (1) scaling all of the curves on the same axis and (2) the symmetry within silica which leads to a decrease in the intensity of this peak relative to the asymmetry when Si−O−C bonds are present in the hybrids.[53] Higher intensities of TP_{231a} and TP_{321a} fibers in the FTIR spectral region of 3300 cm^{-1} means they have more −OH groups than TP_{411a} and TP_{111a}. The presence of a larger number of −OH groups may be due to hydrolysis of TEOS yielding Si−OH and possibly because some of the PVA groups that have not participated in the TEOS cross-linking.

Figure 7 shows the effect of aging time on the FTIR spectra of silica−PVA hybrid fibers. All of the samples in this series

Figure 7. FTIR spectra of silica−PVA composites. The time the TEOS was aged before adding PVA is noted.

were created by combining the same amount of TEOS precursor and PVA solutions; only the aging time of the TEOS solution, before addition of PVA, differs. The peak at 1080 cm^{-1} increases in intensity with the increase in TEOS gelation time which can be attributed to the higher number of Si−O−Si bonds developed due to prolonged aging of TEOS solution before adding the PVA. The peak at 3400 cm^{-1} (corresponding to −OH groups) is the weakest for the silica precursor aged 1 h (sample TP_{411}), while 2, 3, and 4 h aged TEOS solutions yield hybrid fibers with more intense peaks in this spectral region indicative of higher −OH content. This demonstrates that with longer aging times less of the PVA participates in the condensation and cross-linking, leaving a greater number of −OH groups unreacted. Despite the greater

number of uncross-linked −OH groups, the fibers produced with 2−4 h aging time were still water insoluble. In light of the viscosity results for these solutions, which indicate higher viscosity and non-Newtonian behavior for longer aging times, the larger −OH intensity in FTIR indicates that there may be fewer surface silanols available for cross-linking with PVA, which is consistent with scheme I (Supporting Information). In addition, with longer aging times and hence a higher silica network molecular weight there may be reduced mobility in the PVA chains near the PVA−silica cross-link sites. This restriction in mobility prevents nearby −OH groups from reaching other reactive sites and allows potentially long sections of tethered PVA chains to entangle in the solution rather than becoming part of the gel, resulting in the upturn in viscosity at low shear rates (Figure 5A). However, since the PVA molecules are partially cross-linked they remain insoluble.

3.5. Thermal Analysis of Electrospun Fibers. TGA thermograms were compared to determine the PVA content in the as-spun and water-soaked fibers (Figure 8). Upon heating,

Figure 8. Thermograms of PVA−silica composite fibers with varying TEOS:PVA by mass. As-spun fibers are denoted by the subscript "a", while fibers after soaking are denoted by the subscript "s".

silica shows a weight loss of 6%, which can be attributed to the self-condensation reaction of the silanol groups.[55] Degradation of PVA (TP_{010}) by dehydration on the polymer side chain results in the weight loss at 250−350 °C, while the weight loss from 350 to 500 °C occurs as the C−C bonds of the polymer are cleaved.[56,57] Two major weight loss regions, corresponding to degradation of PVA, were evident in hybrid fibers. Thermograms of fibers with different ratios of silica:PVA show that with the increase in PVA content in the electrospun solution the weight loss of the hybrids increases (Figures 8 and 9) and that the weight loss of the fibers is consistent with the PVA content in the electrospun solution (Figure 9). The small deviation from the theoretical weight loss may also be attributed to self-condensation of the silanols, as with the silica fibers. It can also be noted from Figure 8 that compared to hybrid fibers the PVA-only fibers maintain a higher weight at temperatures ranging between 100 and 220 °C; it is possible that in the presence of silica or TEOS the hydrogen bonding within PVA molecules is disturbed, resulting in greater fiber degradation at lower temperatures compared to PVA alone.
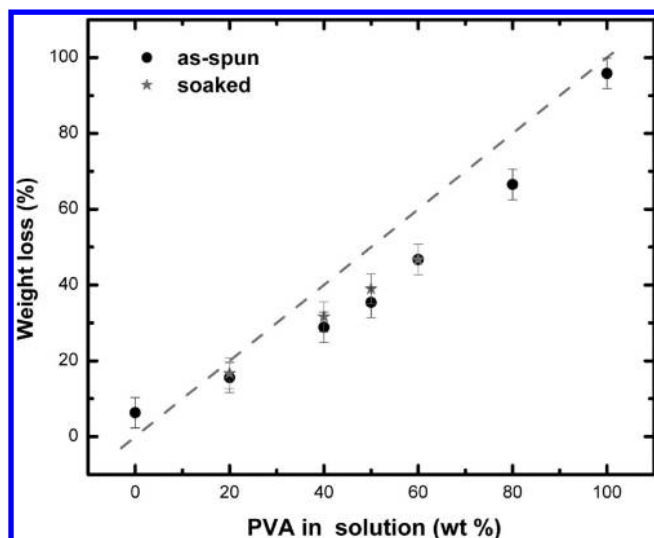
Figure 9. Percent weight loss by 850 °C of as-spun (●) and soaked (★) electrospun fibers measured by TGA. Dashed line indicates a 1:1 correspondence of weight loss to PVA content.

Figure 10. Thermograms of PVA–silica composite fibers (TP$_{411}$– TP$_{414}$). Aging time of the TEOS solution before adding the PVA solution is noted.

Figure 9 compares the TGA weight loss of soaked and unsoaked fibers with varying percentage of TEOS and PVA. Weight losses in the hybrid fibers indicate that, in all cases except TP$_{141}$, virtually none of the PVA was removed by soaking in water. For TP$_{141}$ however, which contains the highest ratio of PVA:silica, the fibers dissolved and fused during the 24-h water exposure, so no TGA for soaked TP$_{141}$ can be reported. This trend indicates that with a higher percentage of PVA in fibers there were fewer PVA molecules involved in the silica network and because they were not cross-linked, they dissolved. Therefore, 2:3 TEOS solution:PVA solution by weight (27:7 TEOS:PVA by weight) may approximately be the minimum critical ratio in which sufficient PVA molecules are cross-linked by the silica network, rendering composite fibers insoluble in water.

To further understand the effect of TEOS gelation on the stability of PVA at higher temperatures, the fibers electrospun at different TEOS aging times were also evaluated by TGA (Figure 10). The onset of weight loss for the sample aged for 4 h (TP$_{414}$) was at a temperature lower than the rest of the fibers, indicating easier removal of some fraction of PVA from the hybrids. Consistent with FTIR results, with longer aging times, there likely remain longer sections of PVA chains or possibly some entire chains that are not cross-linked to the silica network and would likely burn off at a lower temperature. NMR studies of the hybrid fibers will be part of our subsequent work to further elucidate the importance of a critical ratio of TEOS:PVA.

4. CONCLUSIONS

We successfully cross-linked PVA by varying the concentrations and aging times of a silica precursor mixture containing TEOS with a simple electrospinning setup. By varying the TEOS:PVA ratio by mass, nonbeaded hybrid nanofibers were obtained by electrospinning solutions containing as little as 1.4 wt % PVA, compared to 6 wt % PVA which is required without TEOS. The ratio of silica:PVA in solution was found to affect the electrospinnability, fiber morphology, and diameter of fibers due to increasing viscosity and conductivity of the solution. Solutions containing both PVA and TEOS resulted in fibers
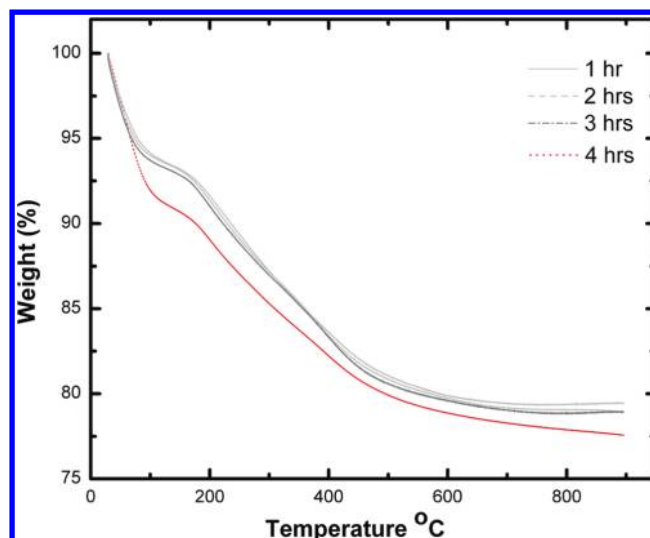
that contained PVA chains cross-linked to the silica network via Si–O–C–O–Si bridges, which were evident in FTIR spectra of composites. Below TEOS:PVA (by weight) of 27:7, fibers were not sufficiently cross-linked to withstand water exposure. The presence of PVA in fibers after soaking in water was confirmed with TGA analysis of weight loss of fibers before and after water exposure. However, the presence of silica in the composite fibers did lower the onset temperature for PVA degradation by 100 °C or more, which is presumably due to an interruption of intramolecular interactions in the PVA. Increased aging time of the TEOS precursor solution, before adding PVA, resulted in a higher solution viscosity that increased the fiber diameter. By employing a silica precursor and modulating the ratio of TEOS:PVA, water-insoluble, silica–PVA hybrid nanofibers were thus electrospun. The resultant nanofibers with their enhanced stability in aqueous media could find applications in fields such as filtration, separation, and tissue engineering.

■ ASSOCIATED CONTENT

Ⓢ Supporting Information

Scheme of hydrolysis and condensation reactions of silica sol, electrospun PVA-TEOS samples immediately after mixing and 2 h thereafter, and FTIR spectra of PVA, silica, and water-soaked PVA–silica nanofibers. This material is available free of charge via the Internet at http://pubs.acs.org.

■ AUTHOR INFORMATION

Corresponding Author
*E-mail: khan@eos.ncsu.edu; cdsaquing@gmail.com.

Present Address
⊥DuPont Central Research and Development, 200 Powder Mill Road, Wilmington, DE 19880-0304

Author Contributions
§Co-first authors.

Notes
The authors declare no competing financial interest.

REFERENCES

(1) Zou, H.; Wu, S.; Shen, J. Polymer/Silica Nanocomposites: Preparation, Characterization, Properties, and Applications. *Chem. Rev.* **2008**, *108*, 3893−3957.

(2) Shao, C.; Kim, H. Y.; Gong, J.; Ding, B.; Lee, D. R.; Park, S. J. Fiber Mats of Poly(vinyl alcohol)/silica Composite via Electrospinning. *Mater. Lett.* **2003**, *57*, 1579−1584.

(3) Larsen, G.; Velarde-Ortiz, R.; Minchow, K.; Barrero, A.; Loscertales, I. G. A Method for Making Inorganic and Hybrid (Organic/Inorganic) Fibers and Vesicles with Diameters in the Submicrometer and Micrometer Range via Sol-Gel Chemistry and Electrically Forced Liquid Jets. *J. Am. Chem. Soc.* **2003**, *125* (5), 1154−55.

(4) Wu, S.; Li, F.; Wu, Y.; Xu, R.; Li, G. Preparation of Novel Poly(vinyl alcohol)/SiO₂ Composite Nanofiber Membranes with Mesostructure and their Application for Removal of Cu²⁺ from Waste Water. *Chem. Commun.* **2010**, *46*, 1694−1696.

(5) Li, J.; Suo, J.; Deng, R. Structure, Mechanical, and Swelling Behaviors of Poly(vinyl alcohol)/SiO₂ Hybrid. *J. Reinf. Plast. Compos.* **2009**, *29*, 618.

(6) Kulkarni, S. S.; Kittur, A. A.; Aralaguppi, M. I.; Kariduraganavar, M. Y. Synthesis and Characterization of Hybrid Membranes Using Poly(vinyl alcohol) and Tetraethylorthosilicate for the Pervaporation Separation of Water− Isopropanol Mixtures. *J. Appl. Polym. Sci.* **2004**, *94*, 1304−1315.

(7) Chen, L. J.; Liao, J. D.; Lin, S. J.; Chuang, Y. J.; Fu, Y. S. Synthesis and Characterization of PVB/Silica Nanofibers by Electrospinning Process. *Polymer* **2009**, *50*, 3516−3521.

(8) Patel, A. C.; Li, S.; Yuaan, J. M.; Wei, Y. In Situ Encapsulation of Horseradish Peroxidase in Electrospun Porous Silica Fibers for Potential Biosensor Applications. *Nano Lett.* **2006**, *6* (5), 1042−1046.

(9) Xu, Y.; Zhou, W.; Zhang, L.; Cheng, L. Spinnability and Crystallizability of Silica Glass Fiber by the Sol-Gel Method. *J. Mater. Process. Technol.* **2000**, *101*, 44−46.

(10) Peltola, T.; Jokinen, M.; Veittola, S.; Rahiala, H.; Urpo, A. Y. Influence of Sol and Stage of Spinnability on in vitro Bioactivity and Dissolution of Sol-Gel-Derived SiO₂ Fibers. *Biomaterials* **2001**, *22*, 589−598.

(11) Ji, L.; Zhang, X. Ultrafine Polyacrylonitrile/Silica Composite Fibers via Electrospinning. *Mater. Lett.* **2008**, *62*, 2161−2164.

(12) Li, D.; Xia, Y. Electrospinning of Nanofibers: Reinventing the Wheel? *Adv. Mater.* **2004**, *16*, 1151−1170.

(13) Zeleny, J. The electrical Discharge from Liquid Points, and a Hydrostatic Method of Measuring the Electric Intensity at Their Surfaces. *Phys. Rev.* **1914**, *3* (2), 69−91.

(14) Greiner, A.; Wendorff, J. H. Electrospinning: A Fascinating Method for the Preparation of Ultrathin Fibers. *Angew. Chem., Int. Ed.* **2007**, *46*, 5670−5703.

(15) Taylor, G. Disintegration of Water Drops in an Electric Field. *Proc. R. Soc. London, Ser. A* **1964**, *280*, 383−397.

(16) Saquing, C.; Manasco, J. L.; Khan, S. A. Electrospun Nanoparticle−Nanofiber Composites via a One-Step Synthesis. *Small* **2009**, *5*, 944−951.

(17) Gopal, R.; Kaur, S.; Ma, Z. W.; Chan, C.; Ramakrishna, S.; Matsuura, T. Electrospun Nanofibrous Filtration Membrane. *J. Membr. Sci.* **2006**, *281* (1−2), 581−586.

(18) Qi, H.; Hu, P.; Xu, J.; Wang, A. Encapsulation of Drug Reservoirs in Fibers by Emulsion Electrospinning: Morphology Characterization and Preliminary Release Assessment. *Biomacromolecules* **2006**, *7* (8), 2327−2330.

(19) Bhardwaj, N.; Kundu, S. C.; Electrospinning, A Fascinating Fiber Fabrication Technique. *Biotechnol. Adv.* **2010**, *28* (3), 325−347.

(20) Wu, Y.; Dong, Z.; Wilson, S.; Clark, R. L. Template Assited Assembly of Electrospun Fibers. *Polymer* **2010**, *51* (14), 3244−3248.

(21) Cheng, C.; Chen, J.; Chen, F.; Hu, P.; Wu, X. F.; Reneker, D. H.; Hou, H. High-Strength and High-Toughness Polyimide Nanofibers: Synthesis and Characterization. *J. Appl. Polym. Sci.* **2010**, *116* (3), 1581−1586.

(22) Ramaseshan, R.; Sundrrajan, S.; Jose, R.; Ramakrishna, S. Nanostructured Ceramics by Electrospinning. *J. Appl. Phys.* **2007**, *102*, 111101.

(23) Burgar, C.; Hsiao, B. S.; Chu, B. Nanofibrous Materials and Their Applications. *Annu. Rev. Mater. Res.* **2006**, *36*, 333−68.

(24) Brinker, C. J.; Scherer, G. W. *Sol-Gel Science, The Physics and Chemistry of Sol-gel Processing*; Academic Press: New York, 1990.

(25) Landry, C. J. T.; Coltrain, B. K.; Wesson, J. A.; Zumbulyadis, N.; Lippert, J. A. In-Situ Polymerization of Tetraethoxysilane in polymers: Chemical Nature of the Interactions. *Polymer* **1992**, *33* (7), 1496−1506.

(26) Choi, S. S.; Lee, S. G.; Im, S. S.; Kim, S. H.; Joo, Y. L. Silica Nanofibers from Electrospinning/Sol-Gel Process. *J. Mater. Sci. Lett.* **2003**, *22*, 891−893.

(27) Xu, X.; Guo, G.; Fan, Y. Fabrication and Characterization of Dense Zirconia and Zirconia-Silica Ceramic Nanofibers. *J. Nanosci. Nanotechnol.* **2010**, *10* (9), 5672−5679.

(28) Wu, Y.-n.; Li, F.; Wu, Y.; Jia, W.; Hannam, P.; Qiao, J.; Li, G. Formation of Silica Nanofibers with Hierarchical Structure via Electrospinning. *Colloid Polym. Sci.* **2011**, *289*, 1253−1260.

(29) Hassan, C. M.; Peppas, N. A. Structure and Applications of Poly(vinyl alcohol) Hydrogels produced by Conventional Crosslinking or by Freezing/Thawing Methods. *Adv. Polym. Sci.* **2000**, *153*, 37−65.

(30) Wang, X.; Fang, D.; Yoon, K.; Hsiao, B. S.; Chu, B. High Performance Ultrafiltration Composite Membranes based on Poly(vinyl alcohol) Hydrogel Coating on Crosslinked Nanofibrous Poly(vinyl alcohol) Scaffold. *J. Membr. Sci.* **2006**, *278*, 261−268.

(31) Xiao, S.; Feng, X.; Huang, R. Y.M. Investigation of Sorption Properties and Pervaporation Behaviors under Different Operating Conditions for Trimesoyl Chloride-Crosslinked PVA Membranes. *J. Membr. Sci.* **2007**, *302* (1−2), 36−44.

(32) Jenni, A.; Holzer, L.; Zurbriggen, R.; Herwegh, M. Influence of Polymers on Microstructure and Adhesive Strength of Cementitious Tile Adhesive Mortars. *Cem. Concr. Res.* **2005**, *35* (1), 35−50.

(33) Krumova, M.; Lopez, D.; Benavente, R.; Mijangos, C.; Perena, J. M. Effect of Crosslinking on the Mechanical and Thermal Properties of Poly(vinyl alcohol). *Polymer* **2000**, *41* (26), 9265−9272.

(34) Nuttelman, C. R.; Henry, S. M.; Anseth, K. S. Synthesis and Characterization of Photocrosslinkable, Degradable Poly(vinyl alcohol)-based Tissue Engineering Scaffolds. *Biomaterials* **2002**, *23* (17), 3617−3626.

(35) Tang, C.; Saquing, C. D.; Harding, J. R.; Khan, S. A. In Situ Cross-Linking of Electrospun Poly(vinyl alcohol) Nanofibers. *Macromolecules* **2010**, *43*, 630−637.

(36) Kurkuri, M. D.; Aminabhavi, T. M. Poly(vinyl alcohol) and Poly(acrylic acid) Sequential Interpenetrating Network pH Sensitive Microspheres for the Delivery of Diclofenac Sodium to the intestine. *J. Controlled Release* **2004**, *96* (1), 9−20.

(37) Stauffer, S. R.; Peppast, N. A. Poly(vinyl alcohol) Hydrogels prepared by Freezing-Thawing Cyclic Processing. *Polymer* **1992**, *33* (18), 3932−3936.

(38) Cho, D.; Hoepker, N.; Frey, M. W. Fabrication and Characterization of Conducting Polyvinyl Alcohol Nanofibers. *Mater. Lett.* **2012**, *68* (1), 293−295.

(39) Yuan, J.; Mo, H.; Wang, M.; Li, L.; Zhang, J.; Shen, J. Reactive Electrospinning of Poly(vinyl alcohol) Nanofibers. *J. Appl. Polym. Sci.* **2012**, *12* (2), 1067−1073.

(40) Qin, X.-H.; Wang, S.-Y. Electrospun Nanofibers from Crosslinked Poly(vinyl alcohol) and Its Filtration Efficiency. *J. Appl. Polym. Sci.* **2008**, *109* (2), 951−956.

(41) Rigby, S. P.; Fairhead, M.; Walle, C. F. Engineering Silica Particles as Oral Drug Delivery Vehicles. *Curr. Pharm. Design* **2008**, *14*, 1821−1831.

(42) Rosenholm, J. M.; Linden, M. Towards Establishing Structure-Activity Relationships for Mesoporous Silica in Drug Delivery Applications. *J. Controlled Release* **2008**, *128*, 157−164.

(43) Li, J.; Suo, J.; Deng, R. Structure, Mechanical, and Swelling Behaviors of Poly(vinyl alcohol)/SiO$_2$ Hybrid. *J. Reinf. Plast. Compos.* **2010**, *29* (4), 618−629.

(44) Guo, M.; Ding, B.; Li, X.; Wang, X.; Yu, J.; Wang, M. Amphiphobic Nanofibrous Silica Mats with Flexible and High-Heat-Resistant Properties. *J. Phys. Chem. C* **2010**, *114*, 916−921.

(45) Jin, Y.; Yang, D.; Kang, D.; Jiang, X. Fabrication of Necklace-like Structures via Electrospinning. *Langmuir* **2010**, *26* (2), 1186−1190.

(46) Kanehata, M.; Ding, B.; Shiratori, S. Nanoporous Ultra-high Specific Surface Inorganic Fibres. *Nanotechnology* **2007**, *18*, 315602.

(47) Srinivasan, D.; Rao, R.; Zribi, A. Synthesis of Novel Micro- and Mesoporous Zeolite Nanostructures Using Electrospinning Techniques. *J. Electron Mater.* **2006**, *35* (3), 504−509.

(48) Bandyopadhyay, A.; Sarkar, M. D.; Bhowmick, A. K. Structure-Property Relationship in Sol-Gel Derived Polymer/Silica Hybrid Nanocomposites prepared at Various pH. *J. Mater. Sci.* **2006**, *41*, 5981−5993.

(49) Koski, A.; Yim, K.; Shivkumar, S. Effect of Molecular Weight on Fibrous PVA produced by Electrospinning. *Mater. Lett.* **2004**, *58*, 493−497.

(50) Liu, S.; Zhang, Z.; Zhang, H.; Zhang, Y.; Wei, S.; Ren, L.; Wang, C.; He, Y.; Li, F.; Xiao, F. S. Phase separation of Organic/Inorganic Hybrids induced by Calcination: A Novel Route for Synthesizing Mesoporous Silica and Carbon Materials. *J. Colloid Interface Sci.* **2010**, *345*, 257−261.

(51) Mansur, H. S.; Sadahira, C. M.; Souza, A. N.; Mansur, A. A. P. FTIR Spectroscopy Characterization of Poly (vinyl alcohol) Hydrogel with Different Hydrolysis Degree and Chemically Crosslinked with Glutaraldehyde. *Mater. Sci. Eng., C* **2008**, *28* (4), 539−548.

(52) Andrade, G. I.; Barbosa-Stancioli, E. F.; Mansur, A. A. P.; Vasconcelos, W. L.; Mansur, H. S. Small-angle X-ray Scattering and FTIR Characterization of Nanostructured Poly (vinyl alcohol)/Silicate Hybrids for Immunoassay Applications. *J. Mater. Sci.* **2008**, *43*, 450−463.

(53) Banwell, C. N. *Fundamental of Molecular Spectroscopy*, 3rd ed.; McGRAW-HILL Book Company (U.K.) Limited: London, 1983.

(54) Xu, Y.; Li, Z. H.; Fan, W. H.; Wu, D.; Sun, Y.; Rong, L.; Dong, B. Density fluctuation in silica−PVA hybrid gels determined by small-angle X-ray scattering. *Appl. Surf. Sci.* **2004**, *225* (1−4), 116−123.

(55) Huang, W. L.; Cui, S. H.; Liang, K. M.; Yuan, Z. F.; Gu, S. R. Evolution of Pore and Surface Characteristics of Silica Xerogels during Calcining. *J. Phys. Chem. Solids* **2002**, *63*, 645.

(56) Nakane, K.; Yamashita, T.; Iwakura, K.; Suzuki, F. Properties and Structure of Poly(vinyl alcohol)/Silica Composites. *J. Appl. Polym. Sci.* **1999**, *74*, 133−138.

(57) Suzuki, F.; Nakane, K.; Piao, J. S. Formation of a Compatible Composite of Silica/Poly(vinyl alcohol) through the Sol-Gel Process and a Calcinated Product of the Composite. *J. Mater. Sci.* **1996**, *31*, 1335−1340.